olefinic double bond in the $\pi$-electron bridge could lead to significant improvement in the thermal stability of the chromophore without a sacrifice of its optical nonlinearity (17).

Accordingly, we synthesized **6,** in which one of the double bonds in the polyene bridge was replaced by a thiophene ring, by a reaction analogous to that used for **5** and characterized the compound by $^1$H NMR and elemental analysis. Interestingly, **6** retained the excellent solubility observed for **5** and had a similar absorption maximum in the visible spectrum. EFISH measurements indicated that **6** was somewhat more nonlinear than **5**, as seen in Table 1. Compound **6** showed no significant decomposition after heating in methylnaphthalene at 150°C for 20 min (less than 5%) and less than 10% decomposition after heating at 200°C for 20 min. Thus, these results suggest that it is possible to develop chromophores with high optical nonlinearity and adequate thermal stability and to permit their incorporation into high-$T_g$ polymers.

Our results suggest that the [3-(dicyanomethylidene)-2,3-dihydrobenzothiophen-2-ylidene-1,1-dioxide] acceptor is sufficiently powerful to lead to very large values of $\mu\beta$ for several extended dialkylaminophenyl-substituted chromophores. In addition, the $r_{33}$ value reported here is significantly larger than any value that has been reported to date for a poled polymer and almost twice that of lithium niobate. Molecules can be synthesized that have not only large nonlinearities but also reasonable stability at 200°C. Although much additional work must be done before commercially viable electro-optic polymers with such large $r_{33}$ values become available, these results show that organic polymers can have substantially larger optical nonlinearities than lithium niobate.

### REFERENCES AND NOTES


1. D. S. Chemla and J. Zyss, Eds., *Nonlinear Optical Properties of Organic Molecules and Crystals*, vols. 1 and 2 (Academic Press, San Diego, 1987).
2. S. R. Marder, J. E. Sohn, G. D. Stucky, Eds., *Materials for Nonlinear Optics: Chemical Perspectives*, vol. 455 of the *ACS Symposium Series* (American Chemical Society, Washington, DC, 1991).
3. S. R. Marder and J. W. Perry, *Science* **263**, 1706 (1994).
4. A. Yariv and P. Yeh, *Optical Waves in Crystals* (Wiley, New York, 1984).
5. C. B. Gorman and S. R. Marder, *Proc. Natl. Acad. Sci. U.S.A.* **90**, 11297 (1993).
6. G. Bourhill *et al.*, *J. Am. Chem. Soc.* **116**, 2619 (1994).
7. S. R. Marder *et al.*, *Science* **252**, 103 (1991).
8. W. Baumann, French Patent Fr2438045 (1980).
9. P. A. Cahill and K. D. Singer, *ACS Symp. Ser.* **455**, 200 (1991).
10. J. March, *Advanced Organic Chemistry: Reaction Mechanisms and Structure* (Wiley Interscience, New York, 1985).
11. S. R. Marder *et al.*, *Science* **263**, 511 (1994).
12. V. P. Rao, A. K. Jen, K. Wong, R. M. Mininni, *Proc. Soc. Photo-Opt. Instrum. Eng.* **1775**, 32 (1993).
13. P. Rao, A. K.-Y. Jen, K. Y. Wong, K. J. Drost, *J. Chem. Soc. Chem. Commun.* 1118 (1993).
14. G. R. Möhlmann *et al.*, *Proc. Soc. Photo-Opt. Instrum. Eng.* **1337**, 215 (1990).
15. C. C. Teng and H. T. Man, *Appl. Phys. Lett.* **56**, 1734 (1989).
16. Comparison of materials for electro-optic applications can be more meaningfully gauged by the electro-optically induced change in phase, $\Delta\Phi$, of a light beam passing through the material, which is given by

$$\Delta\Phi = (\pi/\lambda)\Delta nL = (\pi/\lambda)n^3r_{33}EL$$

where $\lambda$ is the wavelength of light being modulated, $L$ is the propagation distance over which the beam is being modulated, $n$ is the refractive index, and $E$ is the applied external field. Thus, considering the phase change per unit electric field, a useful figure of merit would be $n^3r_{33}$. For lithium niobate, $n^3r_{33}$ is ~300 pm/V (4) and for a reasonable $n$ of ~1.7 for our polymer, $n^3r_{33}$ would be ~270 pm/V, similar to the value for lithium niobate. Further considerations show that a figure of merit characterizing high-frequency power consumption is given by $n^3r_{33}/\varepsilon$ (where $\varepsilon$ is the dielectric constant). For electro-optic polymers (2), $\varepsilon$ is conservatively <6. In contrast, lithium niobate has a value of $\varepsilon$ of 28 (4); thus, considering the figure of merit for power consumption, the polymer would be much more efficient.
17. S. Gilmour *et al.*, *Chem. Mater.* **6**, 1603 (1994).
18. J. L. Oudar and D. S. Chemla, *J. Chem. Phys.* **66**, 2664 (1977).



19. The work in this paper was performed in part at the Center for Space Microelectronics Technology, Jet Propulsion Laboratory, California Institute of Technology, under contract with the National Aeronautics and Space Administration. This work was sponsored by the Ballistic Missile Defense Organization, Innovative Science and Technology Office. Support from the National Science Foundation and the Air Force Office of Scientific Research is also gratefully acknowledged. M.S. thanks the Schweiz Nationalfonds for support. P.V.B. thanks the James Irvine Foundation for a postdoctoral fellowship.

9 August 1995; accepted 7 November 1995


# Chaos and the Shapes of Elliptical Galaxies

David Merritt

Hubble Space Telescope observations reveal that the density of stars in most elliptical galaxies rises toward the center in a power-law cusp. Many of these galaxies also contain central dark objects, possibly supermassive black holes. The gravitational force from a steep cusp or black hole will destroy most of the box orbits that constitute the "backbone" of a triaxial stellar system. Detailed modeling demonstrates that the resulting chaos can preclude a self-consistent, strongly triaxial equilibrium. Most elliptical galaxies may therefore be nearly axisymmetric, either oblate or prolate.

Information about the three-dimensional shape of a galaxy is lost when the galaxy is projected onto the plane of the sky. This loss of information is acute in the case of elliptical galaxies, whose apparent shapes are elliptical but whose intrinsic shapes could be oblate, prolate, or fully triaxial. Before about 1975, elliptical galaxies were thought to be rotationally flattened oblate spheroids. The discovery that elliptical galaxies rotate much more slowly than does a fluid body with the same shape (1) led to the hypothesis that most of these systems are triaxial ellipsoids, with shapes that are maintained by anisotropic velocity dispersions rather than by centrifugal force (2). The triaxial hypothesis was supported by the successful construction of self-consistent triaxial models on the computer (3). Most of the stars in these numerical models occupied "regular" orbits that respect three isolating integrals, two in addition to the energy; the major families of regular orbits are the short- and long-axis "tubes" and the "boxes" (4).

Box orbits are uniquely associated with the triaxial geometry; they densely fill a box- or bow tie–shaped region, and a star on such an orbit passes arbitrarily close to the galaxy center after many oscillations. The time-averaged shape of a box orbit mimics that of the underlying galaxy, and the potential from a star on a box orbit helps to support the triaxial shape of the galaxy as a whole. Box orbits are always found to be strongly populated in the self-consistent triaxial models. They exist only in triaxial potentials with "cores," that is, models in which the density near the center is approximately constant and the corresponding gravitational potential is roughly quadratic in the coordinates (5).

Recent Hubble Space Telescope observations of the centers of elliptical galaxies (6) reveal that these galaxies almost never have constant-density cores; the stellar density always continues to rise, roughly as a power law, toward the smallest observable radius. In fainter ellipticals, the stellar density $\rho$ increases roughly as $\rho \propto r^{-2}$, whereas for brighter ellipticals the cusp slope is $\rho \propto r^{-1}$ or shallower (7). In addition, there is increasingly strong evidence for massive dark objects (MDOs), possibly supermassive black holes, at the centers of many elliptical galaxies (8). In the most convincing cases, these central singularities appear to contain as much as 1% of the total mass of the galaxy.

Department of Physics and Astronomy, Rutgers University, Piscataway, NJ 08855, USA.

A central mass concentration can strongly perturb the motion of a star on a box orbit, regardless of its apocenter distance, because a star on such an orbit eventually will pass arbitrarily close to the center and be deflected by the strong gravitational force there (9). The result is a sensitive dependence of the orbital trajectory on initial conditions; in other words, the orbit loses its two nonclassical integrals of motion and becomes chaotic. The degree of chaos can be quantified by means of the Liapunov characteristic numbers that measure the average rate of exponential divergence of two initially nearby trajectories. Fig. 1A shows histograms of Liapunov numbers for ensembles of boxlike orbits (defined as orbits that have a stationary point) at one energy in a triaxial model with the density law

$$\rho(m) = \rho_0(m^2 + m_0^2)^{-1}(1 + m^2)^{-1}$$

$$m^2 = \frac{x^2}{a^2} + \frac{y^2}{b^2} + \frac{z^2}{c^2} \qquad (1)$$

with $c/a = 0.5$ and $b/a = 0.79$; $x$, $y$, and $x$ are spatial coordinates and $m$ defines the isodensity surfaces. The parameter $m_0$ is a "core radius"; when $m_0 = 1$, Eq. 1 reduces to the "perfect ellipsoid" in which all orbits are regular (*10*), whereas for small $m_0$, this density law has an $r^{-2}$ central cusp similar to those observed in many elliptical galaxies.

When $m_0 < 10^{-1}$, most of the boxlike orbits are chaotic; the only exceptions are orbits that lie close to stable, resonant orbits that avoid the center (Fig. 2A). The destruction of the box orbits also occurs in models with a central singularity or black hole (Figs. 1B and 2B). In both cases, the typical Liapunov time scale for the divergence of nearby trajectories is three to five times the oscillation period of the long-axis closed orbit of the same energy; this period is defined as the dynamical time (Table 1). Stars in the central regions of elliptical galaxies have made $10^2$ to $10^3$ radial oscillations since the epoch of galaxy formation; thus, elliptical galaxies are many Liapunov times old.

A star on a chaotic orbit will eventually visit every point in configuration space consistent with energy conservation; it will fill a region inside of the equipotential surface corresponding to its energy. These surfaces are more nearly spherical than the equidensity surfaces that define the galaxy figure; hence, chaotic orbits are less useful than regular box orbits for building self-consistent models. However, even chaotic orbits have structure. Fig. 3 illustrates the density of an ensemble of stars that fills chaotic phase space in an approximately time-independent way at one energy. The shape is similar to that of a superposition of boxlike orbits, because the chaotic trajectory fills the part of phase space that would have been occupied by box orbits in a fully integrable model. However, because the chaotic phase space at a given energy is interconnected through the "Arnold web" (*11*), there exists just a single invariant density at each energy, as shown in Fig. 3.

The "mixing time" of a chaotic orbit may be defined as the time required for an ensemble of stars on that orbit to reach a fully mixed state like that of Fig. 3. In a real galaxy, the mixing process is likely to be extremely complex, involving violent collapse and rapidly varying forces during galaxy formation (*12*). However, we can place an upper limit on the mixing time by asking how much time is required for an ensemble of stars in the chaotic phase space of a time-independent potential to fill its allowed phase-space region in a nearly uniform way. Numerical experiments show that this relaxation process is roughly exponential, with a time constant of ~100 dynamical times in triaxial potentials with steep cusps or massive central singularities (*13*). After a few hundred dynamical times, the density in the chaotic phase-space region achieves a nearly constant, coarse-grained value and ceases to evolve. We would therefore expect the chaotic orbits in at least the central regions of a triaxial galaxy with a strong central mass concentration to be fully mixed.

The invariant distribution of Fig. 3 plays the role of a single orbit; it represents an unchanging and irreducible distribution of stars and can be used as a building block for a self-consistent model. However, unlike the regular orbits (which respect three integrals of the motion and therefore comprise a two-parameter family at every energy), there is only one invariant density at each energy in chaotic phase space. The replacement of the regular box orbits by chaotic trajectories thus limits the freedom to construct a self-consistent model, because it effectively reduces the number of different orbits. This limitation does not exist in oblate or prolate geometries, however, because axisymmetric potentials support only tube orbits, all of which avoid the center and most of which remain regular. Thus, the nonexistence of a triaxial equilibrium with a given density profile would imply that a galaxy with the same mass distribution must be either axisymmetric or in the process of evolving toward an axisymmetric state.

The degree to which chaos limits the freedom to construct triaxial equilibria was explored by means of two models with Dehnen's (*14*) density law,

$$\rho(m) = \rho_0 m^{-\gamma}(1 + m)^{-(4-\gamma)} \qquad (2)$$

where $\gamma$ is the logarithmic slope of the central density profile. The first model explored (the "strong cusp" model) had $\gamma \approx 2$, corresponding to fainter elliptical galaxies such as M32. The "weak cusp" model had $\gamma \approx 1$, a good description of brighter ellipticals such as M87. The axis ratios selected were $c/a = 0.5$ and $b/a = 0.79$. A total of 7000 orbits were integrated for 100

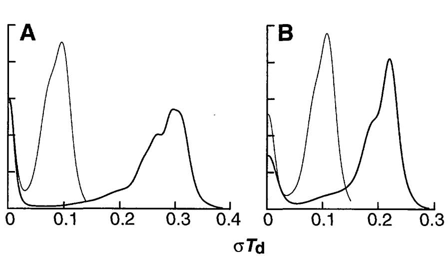


**Fig. 1.** Histograms of Liapunov numbers for isoenergetic ensembles of boxlike orbits in triaxial potentials. Starting points for the orbits were chosen from a uniform grid on an equipotential surface near the half-mass radius of the model (Fig. 2). Each orbit was integrated for $10^4$ dynamical times $T_d$; the thick and thin curves represent the largest Liapunov number $\sigma_1$ and the second Liapunov number $\sigma_2$, respectively. Regular orbits lie in the narrow peaks near $\sigma T_d = 0$. (**A**) $m_0 = 10^{-3}$; (**B**) $m_0 = 10^{-1}$, and a central point mass containing 0.3% of the total galaxy mass has been added.

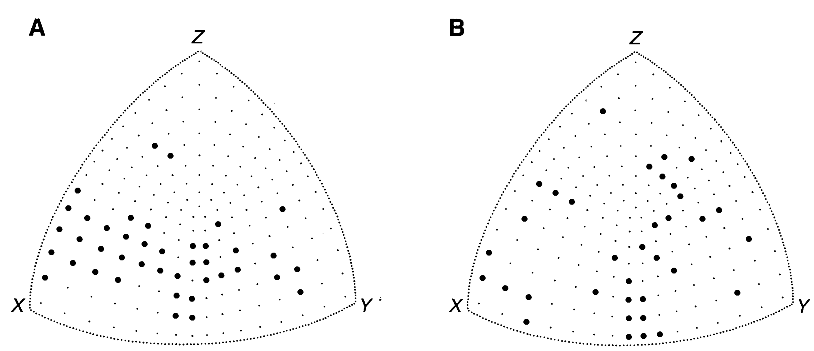


**Fig. 2.** (**A** and **B**) Starting points of the regular and chaotic orbits whose Liapunov numbers make up the histograms of Fig. 1, A and B, respectively. Each dot represents an initial point on one octant of the equipotential surface; small dots are chaotic orbits and large dots are regular orbits. Every orbit was dropped with zero velocity from this surface. The $X$ and $Z$ axes are the long and short axes, respectively.

dynamical times in each of the models, and their time-averaged densities were stored in a grid of $10^3$ cells. A quadratic-programming algorithm was then used to find a set of nonnegative orbital weights that reproduced the known mass of the model in the cells (*15*).

Attempts to construct self-consistent solutions using just the regular orbits failed for both mass models. Quasi-equilibrium solutions—in which chaotic orbits, computed for only 100 orbital periods, were included with arbitrary orbital weights—were found to exist for both the weak- and strong-cusp models. However, real galaxies constructed in this way would evolve near the center as the chaotic orbits mixed toward their invariant distributions at each energy (*16*).

More nearly stationary solutions were successfully constructed for the weak-cusp mass model; all of the chaotic orbits within the inner half-mass radius could be replaced by the smaller set of invariant distributions without violating self-consistency. However, these models could not be made fully mixed at both large and small radii. No appreciable fraction of the mass could be placed on fully mixed chaotic orbits in the strong-cusp model without driving the solution away from self-consistency. The greater freedom to find solutions in the weak-cusp case resulted from the larger number of regular orbit families in this potential, which allowed less weight to be placed on the chaotic orbits.

These attempts to find self-consistent equilibria were based on only two strongly triaxial mass models; more nearly axisymmetric models with the same density profile would presumably be easier to construct. However, these results demonstrate that chaos can severely reduce the size of solution space for triaxial models and, at least in some cases, preclude self-consistent equilibria.

Although no attempts have yet been made to construct self-consistent triaxial models with central black holes, the results in Figs. 1 and 2 suggest that chaos would constrain such solutions about as strongly as it constrains triaxial models with steep density cusps. Secure detections of MDOs have been made in at least two elliptical galaxies (*17*, *18*); the kinematical signature in both cases was a high streaming velocity of stars or gas very near the center. In addition, strong kinematical evidence for MDOs has been found in a number of S0 galaxies and spirals with bulges (*8*). The failure to detect MDOs in some ellipticals may be attributable to the lack of a rotating subpopulation, or to the fact that the galaxy is not oriented in such a way that the rotation is easily observed. The average mass of the MDOs in these galaxies is ~0.0045 when expressed in units of the total stellar mass of the galaxy. This is close to the average mass required per galaxy if MDOs are dead quasars (*19*), which suggests that most or all ellipticals may harbor nuclear black holes.

**Table 1.** Liapunov numbers of boxlike orbits in triaxial potentials. Orbits were computed for $10^4$ dynamical times at the half-mass energy in the potential corresponding to Eq. 1, with $c/a = 0.5$ and $b/a = 0.79$. Liapunov numbers $\sigma_1$ and $\sigma_2$ are given in units of the dynamical time; $M_{BH}$ represents black hole mass in units of the total mass of the model.

| $m_0$ | $M_{BH}$ | $\sigma_1$ | $\sigma_2$ |
|---|---|---|---|
| $10^{-1}$ | – | $0.14 \pm 0.06$ | $0.045 \pm 0.02$ |
| $10^{-2}$ | – | $0.21 \pm 0.09$ | $0.078 \pm 0.03$ |
| $10^{-3}$ | – | $0.27 \pm 0.05$ | $0.085 \pm 0.02$ |
| $10^{-1}$ | $10^{-3}$ | $0.15 \pm 0.03$ | $0.066 \pm 0.02$ |
| $10^{-1}$ | $3 \times 10^{-3}$ | $0.20 \pm 0.04$ | $0.097 \pm 0.02$ |
| $10^{-1}$ | $10^{-2}$ | $0.28 \pm 0.08$ | $0.16 \pm 0.04$ |

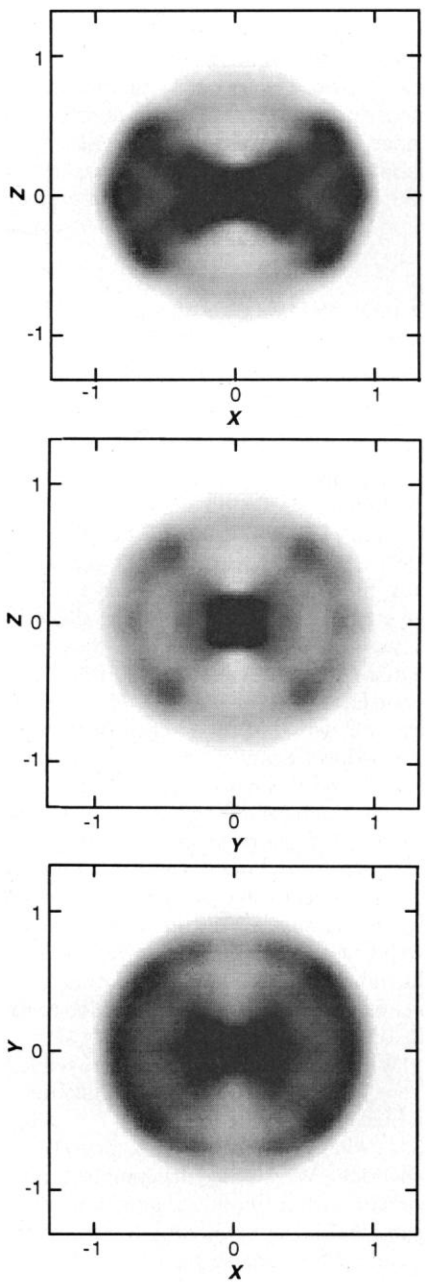


**Fig. 3.** Invariant density of an isoenergetic ensemble of 5000 stars in the chaotic phase space of a triaxial model with $m_0 = 10^{-3}$, $c/a = 0.5$, and $b/a = 0.79$. The *X* and *Z* axes are the long and short axes, respectively, of the triaxial figure. Plotted are the densities near each of the three principal planes.

If most elliptical galaxies contain steep density cusps, nuclear black holes, or both, then the arguments given above suggest that axisymmetry would generally be preferred over triaxiality for these galaxies. This hypothesis would be especially likely to be true for lower luminosity ellipticals, which have the steepest cusps and the shortest dynamical times on average (*6*). The axisymmetric hypothesis is difficult to confirm because no unambiguous test for triaxiality exists. However, most recent studies of elliptical galaxy intrinsic shapes have found that few, if any, elliptical galaxies need to be strongly triaxial (*20*).

The dependence of observed rotation rate on flattening in low-luminosity ellipticals has long been known to be consistent with oblate symmetry for these galaxies (*21*). A classical test for triaxiality is the dependence of major-axis orientation on radius (*22*). Such "isophote twists" are seen in a number of elliptical galaxies, but their interpretation is complicated by the likelihood that some of the twisted galaxies are not relaxed, whereas in others the twist may result from misaligned disks and bars. A stronger test for triaxiality is the detection of stellar streaming along the apparent minor axis of a galaxy (*22*). Minor axis rotation is rare, however, and a statistical study of the 38 elliptical galaxies for which two-dimensional velocity data are available suggests that the data can be well fit by a distribution in which 60% of galaxies are oblate and 40% are prolate (*23*).

The shapes of a few elliptical galaxies have been constrained by detailed comparison of numerical models with kinematical data. The best example is M32, the dwarf companion to the Andromeda galaxy. M32 has a $\rho \propto r^{-1.6}$ stellar cusp and also shows convincing evidence for a MDO containing ~0.25% of the total galaxy mass (*17*); thus, axisymmetry would be expected to be strongly preferred for this galaxy. In fact, oblate models reproduce the detailed kinematics of M32 extremely well (*24*). Rings and disks of gas or dust can sometimes be used as tracers of the shape of the gravitational potential in elliptical galaxies (*25*), although few of these subsystems are both extended and regular enough for the results to be convincing. However, the kinematics of a neutral hydrogen ring surrounding the elliptical galaxy IC 2006 suggest that its dark halo is accurately axisymmetric (26).

Bright ellipticals are observed to be slowly rotating, and if these galaxies are generically axisymmetric, their slow rotation implies nearly equal numbers of stars on tube orbits traveling in both directions. Such a configuration would arise naturally as the potential evolved from triaxiality into axial symmetry by way of the mechanism described here: Stars on boxlike orbits undergo periodic changes in the direction of their angular momenta, and eventually an ensemble of such stars would presumably populate a set of tube orbits with roughly equal numbers of rotating and counterrotating members. A galaxy with this orbital composition might reveal itself by a strongly flattened or double-peaked distribution of line-of-sight velocities (27).

## REFERENCES AND NOTES


1. F. Bertola and M. Capaccioli, *Astrophys. J.* **200**, 439 (1975).
2. J. J. Binney, *Mon. Not. R. Astron. Soc.* **183**, 501 (1978).
3. M. Schwarzschild, *Astrophys. J.* **232**, 236 (1979).
4. For an illustration of the major orbit families in integrable triaxial models, see D. Merritt, *Science* **259**, 1867 (1993).
5. J. Lees and M. Schwarzschild, *Astrophys. J.* **384**, 491 (1992).
6. J. Kormendy *et al.*, in *ESO/OHP Workshop on Dwarf Galaxies,* G. Meylan and P. Prugniel, Eds. (European Southern Observatory, Garching, Germany, 1995), pp. 147–154.
7. D. Merritt and T. Fridman, in *ASP Conf. Ser. Vol. 86, Fresh Views of Elliptical Galaxies,* A. Buzzoni, A. Renzini, A. Serrano, Eds. (Astronomical Society of the Pacific, San Francisco, 1995), pp. 13–21.
8. J. Kormendy and D. Richstone, *Annu. Rev. Astron. Astrophys.* **33**, 581 (1995).
9. O. E. Gerhard and J. J. Binney, *Mon. Not. R. Astron. Soc.* **216**, 467 (1985).
10. G. G. Kuzmin, in *Dynamics of Galaxies and Clusters,* T. B. Omarov, Ed. (Akademie Nauk Kazakh SSR, Alma Ata, 1973), pp. 71–75; P. T. de Zeeuw and D. Lynden-Bell, *Mon. Not. R. Astron. Soc.* **215**, 713 (1985).
11. A. J. Lichtenberg and M. A. Lieberman, *Regular and Stochastic Motion* (Springer-Verlag, New York, 1989).
12. D. Lynden-Bell, *Mon. Not. R. Astron. Soc.* **136**, 101 (1967).
13. D. Merritt and M. Valluri, in preparation.
14. W. Dehnen, *Mon. Not. R. Astron. Soc.* **265**, 250 (1993).
15. D. Merritt and T. Fridman, *Astrophys. J.,* in press.
16. M. Schwarzschild, *ibid.* **409**, 563 (1993).
17. A. Dressler and D. Richstone, *ibid.* **324**, 701 (1988); R. P. van der Marel, T. de Zeeuw, H.-W. Rix, S. D. M. White, *Mon. Not. R. Astron. Soc.* **271**, 99 (1994).
18. R. J. Harms *et al., Astrophys. J.* **435**, L35 (1994).
19. A. Soltan, *Mon. Not. R. Astron. Soc.* **200**, 115 (1982).
20. D. Merritt, in *Morphological and Physical Classification of Galaxies,* G. Longo, M. Capaccioli, G. Busarello, Eds. (Kluwer Academic, Norwell, MA, 1992), pp. 309–320.
21. R. L. Davies, G. Efstathiou, S. M. Fall, G. Illingworth, P. L. Schechter, *Astrophys. J.* **266**, 41 (1983).
22. G. Contopoulos, *Z. Astrophys.* **39**, 126 (1956).
23. M. Franx, G. D. Illingworth, P. T. de Zeeuw, *Astrophys. J.* **383**, 112 (1991).
24. E. E. Qian, P. T. de Zeeuw, C. Hunter, *Mon. Not. R. Astron. Soc.* **274**, 602 (1995).
25. F. Bertola *et al., Astrophys. J.* **373**, 369 (1991).
26. M. Franx and T. de Zeeuw, *ibid.* **392**, L47 (1992).
27. O. Gerhard, *Mon. Not. R. Astron. Soc.* **265**, 213 (1993).


28. I thank M. Valluri for the calculations on which Fig. 3 was based and for helpful comments on the manuscript. S. Tremaine made a number of suggestions that improved the presentation. Supported by NSF grant AST 93-18617 and NASA grant NAG 5-2803.

10 October 1995; accepted 8 December 1995


# Mineralization of Chlorofluorocarbons and Aromatization of Saturated Fluorocarbons by a Convenient Thermal Process


Juan Burdeniuc and Robert H. Crabtree*



**A chemical reaction has been discovered that mineralizes chlorofluorocarbons (CFCs) and enables the complete destruction of these environmentally hazardous species. The reaction products are easily handled solids, including recyclable alkali metal halides. Under milder conditions, the same reaction causes partial defluorination of cyclic perfluoroalkanes to yield perfluoroarenes, which are valuable chemical intermediates. The vaporized substrates are passed over a packed bed of heated sodium oxalate; heating at 270° to 290°C causes mineralization, whereas heating at 230°C causes aromatization.**


Saturated fluorocarbons and CFCs are among the most inert substances known (1). This inertness has environmental consequences because, when released, these species are not destroyed in the lower atmosphere but survive to reach the stratosphere. For example, $CF_4$, released in electrolytic aluminum production, has a high global warming potential through the greenhouse effect (2, 3). CFCs, popular refrigerants, not only have global warming effects but also have a high potential for ozone depletion, because they can release Cl atoms under high-energy ultraviolet photolysis in the ozone layer (3). The same chemical inertness makes it very difficult to effectively dispose of existing stockpiles of CFCs and similar species, and this has been called "a problem of major dimensions" (4, p. 25). Very few reactions of fluorocarbons are known (5); most involve the more reactive fluoroarenes or require corrosive reagents (or reagents that are available only in research quantities). Few of these reactions are applicable to the most refractory saturated species, such as Freons, and none is convenient for routine use on a large scale.

We looked for a two-electron reducing agent, on the grounds that fluoroalkenes are stabler intermediates than are the radicals that would be formed in a one-electron reduction. We wanted to combine the reductant with a fluoride-abstracting component, such as a metal cation. Alkali metal oxalates therefore seemed a good choice. Here, we report an effective and inexpensive method of mineralizing CFCs by passing the vapor through a packed bed of powdered sodium oxalate ($Na_2C_2O_4$) at 270°C, with the use of a vapor-phase multipass apparatus for gases (6) or a reflux multipass apparatus for liquids (7). This reaction, as applied to $CF_2Cl_2$ (Freon-12), is shown in Eq. 1:

$$CF_2Cl_2(g) + 2Na_2C_2O_4(s) = 2NaF(s) + 2NaCl(s) + C(s) + 4CO_2(g) \quad (1)$$

Elemental carbon, which can be isolated and weighed, is formed in the stoichiometric amount expected from Eq. 1. The residue also contains NaCl and NaF in the expected amounts. Very high mineralization yields (8) were obtained from typical Freons (Table 1). No more than three passes were ever required, and for $ClF_2CCF_2Cl$ (Freon-114), even a single pass through the bed caused complete mineralization. This reaction looks promising for the destruction of CFC stockpiles because it requires only very simple hot-tube chemistry, shows no tendency to give uncontrollable exotherms, and uses an inexpensive and noncorrosive reagent. The products (carbon and the al-


Department of Chemistry, Yale University, New Haven, CT 06520–8107, USA.

*To whom correspondence should be addressed.


**Table 1.** Mineralization products of certain perhalocarbons. TM, trap-to-trap multipass apparatus (6); RM, reflux multipass apparatus (7); SP, single-pass apparatus; PS, passes (12). The number of passes required for complete mineralization is given.

| Substrate | Method | PS (no.) | Product yield (%) C | $Cl^-$ | $F^-$ |
|---|---|---|---|---|---|
| $CCl_4$ | RM | – | 99.5 | 100 | – |
| $CFCl_3$ | TM | 2 | 100 | 98.1 | 98.0 |
| $CF_2Cl_2$ | TM | 3 | 100 | 95.0 | 95.0 |
| $ClF_2CCF_2Cl$ | SP | 1 | 96.0 | 100 | 99.0 |